American Journal of Engineering Research (AJER)
e-ISSN: 2320-0847 p-ISSN : 2320-0936
Volume-9, Issue-12, pp-49-55
www.ajer.org
Research Paper Open Access

Effect of contributing shell and nozzle length on pressure capacity

*Walther Stikvoort
Consultant Static Pressure Equipment Integrity
Wagnerlaan 37, 9402 SH, Assen, The Netherlands
** Corresponding Author: Walther Stikvoort*

ABSTRACT: *A simplified limit load type approach known as the pressure area method is often used as a design method for nozzles in pressure vessels. This concept is based on ensuring that the resistive internal force provided by the material is greater than or equal to the reactive load from the applied internal pressure. However, practice shows differences in the contributing length along the vessel shell and the nozzle, which means that this affects the pressure loaded and load bearing area. This article shows the differences in internal pressure capacity depending on the chosen contributing lengths and the associated consequences. The differences found in allowable internal pressure at the nozzle - vessel intersection are to a considerable extent influenced by the selected K_N and K_S factors that determine the contributing (reinforcement) lengths of shell and nozzle neck to be taken into account.*
KEYWORDS: *Limit load, pressure - area method, internal pressure capacity, contributing lengths.*

Date of Submission: 02-12-2020 Date of acceptance: 17-12-2020

I. INTRODUCTION

The principle of the pressure - area method is illustrated by Figure 1. The illustration shows where a certain area of the vessel, in the region of the opening, is multiplied by the design stress. This is equated to the cross - sectional area of the vessel in the same region multiplied by the pressure. The discontinuity stress attenuates with increasing distance from the nozzle - shell junction. The limiting boundary values for the contributing lengths are a function of $\sqrt{(D_o - T)T}$, $\sqrt{(2R_i + T)T}$ and $\sqrt{(d_o - t)t}$ multiplied respectively by an arbitrary factor K_S and K_N, which may differ per design code.
The combinations of the K_S and K_N, which may differ per design code.

The combination of the K_S and K_N values found in different design codes are shown in the table below:

Multiplication factor K_S	Multiplication factor K_N
1.0	1.0
1.0	1.25
0.78	0.78

The background of the limiting boundary values stems from the theory of beams on elastic foundation which deals with discontinuities. Essentially, the "local" stresses at a structural discontinuity will dissipate down to the "general" stress level over some distance related to the damping or attenuation factor β [1][2][3]. The effect of the discontinuity attenuates inverse exponentially with distance. It is noted that the 'die - out' of the stresses in the vicinity of the nozzle-shell junction is a function of the shell radius R divided by β where β can be defined as : $\beta = \frac{1.285}{\sqrt{RT}}$. It will be clear that the reinforcement can only be effective within distances where the discontinuity stresses are acting. The distances from the junction where reinforcement can be utilised for design purposes is limited to be within the 'die - out' or attenuation range.

Because the definition of the effective zone is not very clear - cut, some engineering judgement should be exercised. Depending on the purpose it serves, the effective zone is defined somewhat differently for each type of application. However, they all follow the same pattern based on beams on elastic foundation. Obviously

the 'die - out ' distance depends on which stress resultants or deformation component is being considered. The theory behind this is extensively discussed in numerous textbooks [1],[2],[3],[4] etc.

In addition to the 'die - out' effects described above, Section II below contains a formulation for determining the pressure factor Φ. This pressure factor Φ gives the ratio of the pressure the nozzle - vessel configuration will resist to the pressure the undisturbed shell (w/o nozzle) will resist:

$$\Phi = \frac{\text{pressure resistance of intersecting nozzle}}{\text{pressure resistance of shell w/o nozzle}} \text{ x } 100\%$$

The expression for Φ has been derived from [9]

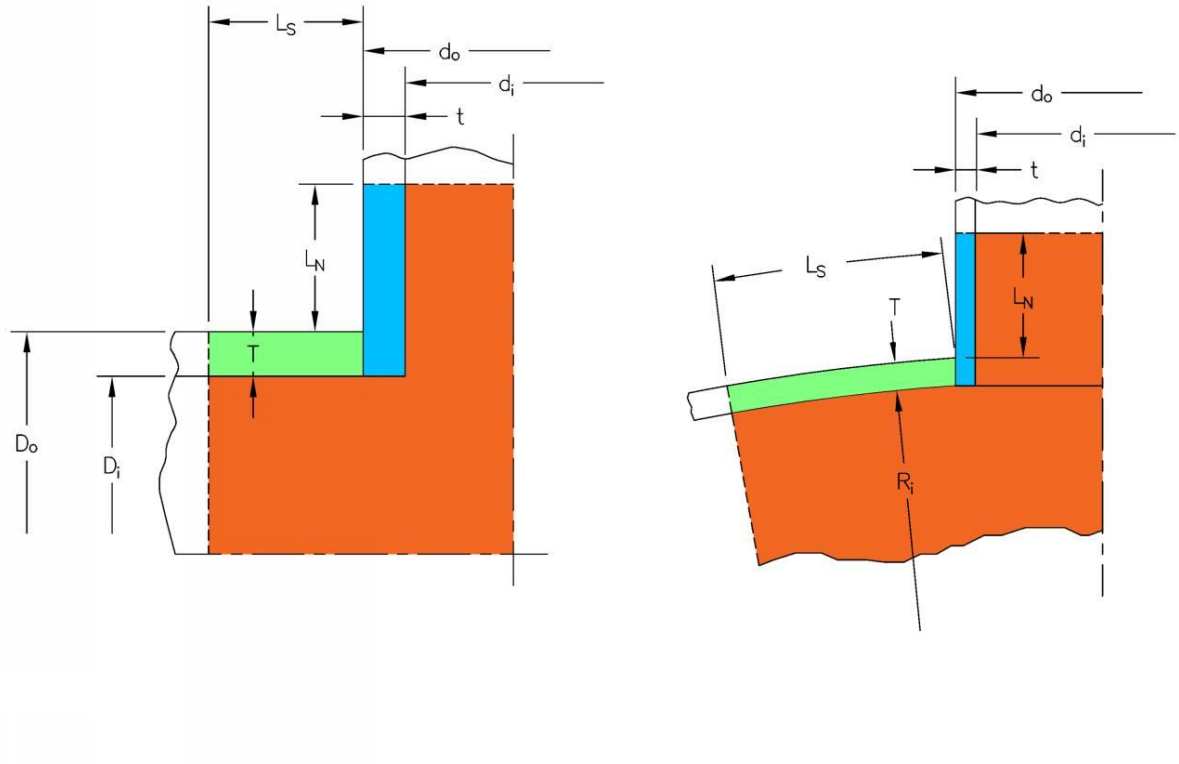

Figure 1: Illustration of flush set - in nozzle configurations in cylindrical and spherical shell

KEY

Discription	Symbol	Color shading code
Pressure loaded area	A_p	
Stress loaded cross-sectional area of shell effective as reinforcement	A_{fs}	
Stress loaded cross-sectional area of nozzle neck effective as reinforcement	A_{fn}	

FORMULA GRID PERTAINING TO FIGURE 1	
Flush set - in nozzle in cylindrical shell	Flush set - in nozzle in spherical shell
$L_S = K_S \sqrt{(D_o - T)\,T}$	$L_S = K_S \sqrt{(2R_i + T)\,T}$
$L_N = K_N \sqrt{(d_o - t)\,t}$	$L_N = K_N \sqrt{(d_o - t)\,t}$
$A_P = \frac{D_i}{2}\left(L_S + \frac{d_o}{2}\right) + \frac{d_i}{2}(L_N + T)$	$A_P = \frac{R_i}{2}\left(L_S + \frac{d_o}{2}\right) + \frac{d_i}{2}(L_N + T)$

$A_{fs} = T\,L_S$	$A_{fs} = T\,L_S$
$A_{fn} = t\,(L_N + T)$	$A_{fn} = t\,(L_N + T)$
MAWP @ nozzle intersection $= \dfrac{f}{\left[\dfrac{A_p}{(A_{fs} + A_{fn})} + 0.5\right]}$	
MAWP undisturbed cylindrical shell: $f.\ln\left[\dfrac{D_o}{D_i}\right]$	MAWP undisturbed spherical shell: $2f.\ln\left[\dfrac{R_i + T}{R_i}\right]$

Remarks:
It is assumed that the design stress (f) of shell and nozzle neck are identical. An approximate method is used for the nozzle in the spherical shell. Simple formulae for calculation of A_p, A_{fs}, and A_{fn} are considered to give acceptable results within the accuracy of the method.

II. SELECTED VESSEL CONFIGURATIONS FOR FURTHER INVESTIGATION

MATERIAL PROPERTIES					
Part	**Material**	**Tensile Strength (MPa)**	**Yield Strength @ 20°C (MPa)**	**Yield Strength @ 250°C (MPa)**	**Design Stress (f) @ 250°C (MPa)**
Cylindrical Shell	A 515 Gr. 65	450	240	198	132
Spherical shell	A 515 Gr. 65	450	240	198	132
Nozzle neck	A 106 Gr. B	415	240	198	132

VESSEL DIMENSIONS						
CASE NUMBER	**CASE #1**	**CASE #2**	**CASE #3**	**CASE #4**	**CASE #5**	**CASE #6**
OD Shell (mm)	2000	2000	2000	-	-	-
ID Sphere radius (mm)	-	-	-	1600	1600	1600
OD Nozzle (mm)	508	508	508	508	508	508
Shell thickness (mm)	10	10	10	10	10	10
Nozzle neck thickness (mm)	13.2	13.2	13.2	13.2	13.2	13.2
K_S	1.0	1.0	0.78	1.0	1.0	0.78
K_N	1.0	1.25	0.78	1.0	1.25	0.78

Note: Net nozzle neck thickness for NPS 20" - S40 = 0.875 x 15.09 = 13.2 mm.

CALCULATION						
CASE NUMBER	**CASE #1**	**CASE #2**	**CASE #3**	**CASE #4**	**CASE #5**	**CASE #6**
L_S (mm)	141.067	141.067	110,0325	179.165	179.165	139.748
L_N (mm)	80.817	101.021	63.037	80.817	101.021	63.037
A_p (mm^2)	413275.7	418205.5	378213.2	368691.3	373621.1	332819.4
A_{fs} (mm^2)	1410.67	1410.67	1100.325	1791.65	1791.65	1397.48
A_{fn} (mm^2)	1198.78	1465.48	964.088	1198.78	1465.48	964.088
MAWP @ intersection (MPa)	0.8308	0.9047	0.7185	1.0663	1.1457	0.933
MAWP w/o nozzle (MPa)	1.3266	1.3266	1.3266	1.6449	1.6449	1.6449

Determination of pressure factor Φ

Φ = Pressure resistance of intersecting nozzle / Pressure resistance of undisturbed shell

For cylindrical shell $\Rightarrow \Phi = \dfrac{(D_o - T)}{T} \times \left[\dfrac{1}{\dfrac{2A_p}{A_f} + 1}\right] \times 100\%$

For sphere $\Rightarrow \Phi = \dfrac{(R_i + T)}{T} \times \left[\dfrac{1}{\dfrac{2A_p}{A_f} + 1}\right] \times 100\%$

$A_f = A_{fs} + A_{fn}$

CALCULATION of PRESSURE FACTOR Φ						
CASE NUMBER	**CASE #1**	**CASE #2**	**CASE #3**	**CASE #4**	**CASE #5**	**CASE #6**
A_p (mm^2)	413275.7	418205.5	378213.2	368691.3	373621.1	332819.4
A_{fs} (mm^2)	1410.67	1410.67	1100.325	1791.65	1791.65	1397.48
A_{fn} (mm^2)	1198.78	1465.48	964.088	1198.78	1465.48	964.088
$A_f = A_{fs} + A_{fn}$ (mm^2)	2609.45	2876.15	2064.413	2990.43	3257.13	2361.568
Φ (%)	62.627	68.195	54.163	65.029	69.873	56.918

III. GRAPHICAL REPRESENTATION OF CALCULATION RESULTS

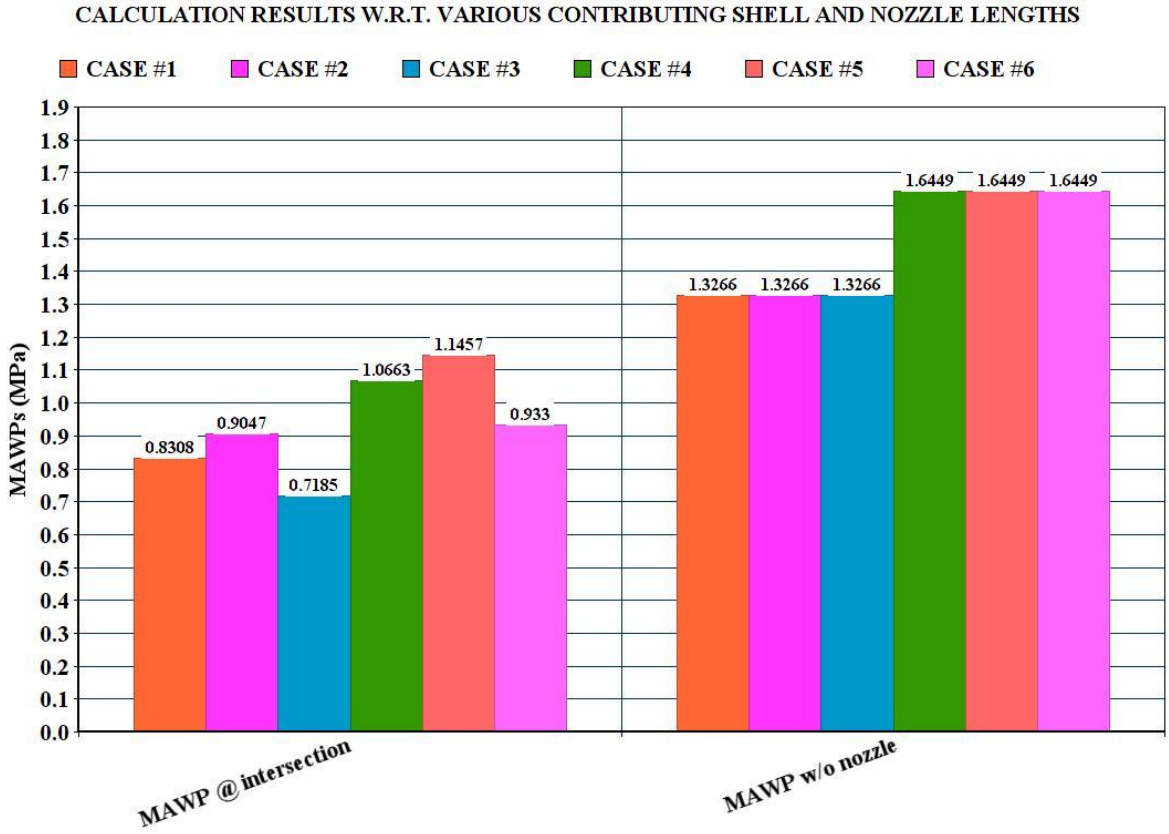

Observations pertaining to performed calculations

It appears from the calculated situations that the lower the K_S and / or K_N values, the lower the allowable internal pressure. On the other hand, the allowable internal pressure increases as the K_S and / or K_N increases. For the nozzle in the cylindrical shell, the maximum difference in allowable pressure found is almost 26% and for the nozzle in the sphere it is approximately 23%. This implies that the most conservative approach is obtained by applying the lowest K_N and K_S values. Of course, different percentages apply to different configurations.

III. DISCUSSION

It has been established that the nozzle intersection is the weakest link in the pressure vessel. By applying a reinforcing pad around the nozzle, the allowable pressure (MAWP) can be increased. To illustrate, this will be elaborated in more detail below. The required dimensions of the reinforcing pads are determined on the basis that the MAWP @ nozzle intersection = MAWP undisturbed cylindrical or spherical shell.

Determination of repad dimensions:

$$A_f = \frac{A_p}{\left[\frac{f}{\text{MA WP w/o nozzle}} - 0.5\right]} \Rightarrow A_{fp} = A_f - A_{fs} - A_{fn} \Rightarrow A_{fp} = W_{pad} \,.\, T_{pad}$$

Assuming $T_{pad} = 1.5\ x\ T$ *we end up with:* $W_{pad} = \frac{A_f - A_{fs} - A_{fn}}{1.5\,T}$

CASE NUMBER	CASE #1	CASE #2	CASE #3	CASE #4	CASE #5	CASE #6
Repad width: Wpad (mm)	104.3	89.9	117.1	108.9	95.2	120.8
Repad thickness: Tpad (mm)	15	15	15	15	15	15

Observation

The cases where $K_S = K_N = 0.78$ follows a reinforcing pad with the largest dimensions. In contrast, the cases with $K_S = 1.0$ and $K_N = 1.25$ have a reinforcing pad with the smallest dimensions. The pad dimensions for $K_S = K_N = 1.0$ are in between. When the repad area is discounted in the formula for the pressure factor Φ, a Φ value of 100% is achieved. The result is that the pressure capacity of the nozzle intersection is the same as that of the undisturbed shell (without nozzle).

To get an impression of the degree of conservatism with regard to the different K_N-K_S scenarios, some numerical finite element analysis (FEA) were performed using ABAQUS software. The MAWPs have been determined sequentially for five selected pad-reinforced nozzle configurations. The results are shown in the table below.

Overview of results of analytical versus numerical computations

MODEL	Number / Symbol	# 1 cylinder	# 2 cylinder	# 3 cylinder	#4 sphere	#5 cylinder
Outside diameter cylindrical or spherical shell (mm)	D_o	1200	1200	3000	4050	1600
Analysis thickness of the shell (mm)	T	12	15	8	25	10
Inside radius of cylindrical or spherical shell (mm)	R_i	588	585	1492	2000	790
Outside nozzle diameter (mm)	d_o	323.8	323.8	609.6	609.6	406.4
Nozzle analysis thickness (mm)	t	8.34	18.76	8.34	15.295	18.76
Internal diameter of nozzle (mm)	d_i	307.12	286.28	592.92	579.01	368.88
Width of reinforcing plate (mm)	W	110	90	145	150	60
Thickness of reinforcing plate (mm)	T_{pad}	12	15	12	25	10
Yield strength of all elements (MPa)	S_y	207	207	207	207	207
MAWP undisturbed shell (MPa)		**2.788**	**3.494**	**0.738**	**3.429**	**1.735**
MAWP FEA (MPa)	P_{FEA}	**2.78**	**3.97**	**0.768**	**2.61**	**1.97**
MAWP : K_N = 1.0 & K_S = 1.0 (MPa)	$P_{1.0;1.0}$	**2.56**	**3.49**	**0.621**	**2.823**	**1.735**
MAWP : K_N = 1.25 & K_S = 1.0 (MPa)	$P_{1.25;1.0}$	**2,614**	**3.493**	**0.645**	**2.89**	**1.735**
MAWP : K_N = 0.78 & K_S = 0.78 (MPa)	$P_{0.78;0.78}$	**2.486**	**3.493**	**0.547**	**2.782**	**1.648**
(P_{FEA} / $P_{1.0;1.0}$)	Ratio	**(1.086)**	**(1.137)**	**(1.237)**	**(0.9245)**	**(1.135)**
(P_{FEA} / $P_{1.25;1.0}$)	Ratio	**(1.0635)**	**(1.1366)**	**(1.191)**	**(0.903)**	**(1.135)**
(P_{FEA} / $P_{0.78;0.78}$)	Ratio	**(1.118)**	**(1.1366)**	**(1.404)**	**(0.938)**	**(1.195)**

Remark

It is interesting to note that in the CODAP [8] the K_S factor is dependent on δ which is defined as:

$$\delta = \frac{d_i}{\sqrt{(D_o - T)\,T}}$$

For $4 \le \delta \le 16$ holds: $K_S = \frac{13}{12} - \frac{\delta}{48}$ while for K_N always a value of 1.0 holds.

This implies that for $\delta \le 4$ a Ks value of 1.0 applies and for $\delta \ge 16$ a value of 0.75 applies. For δ values between 4 and 16, linear interpolation may be used.

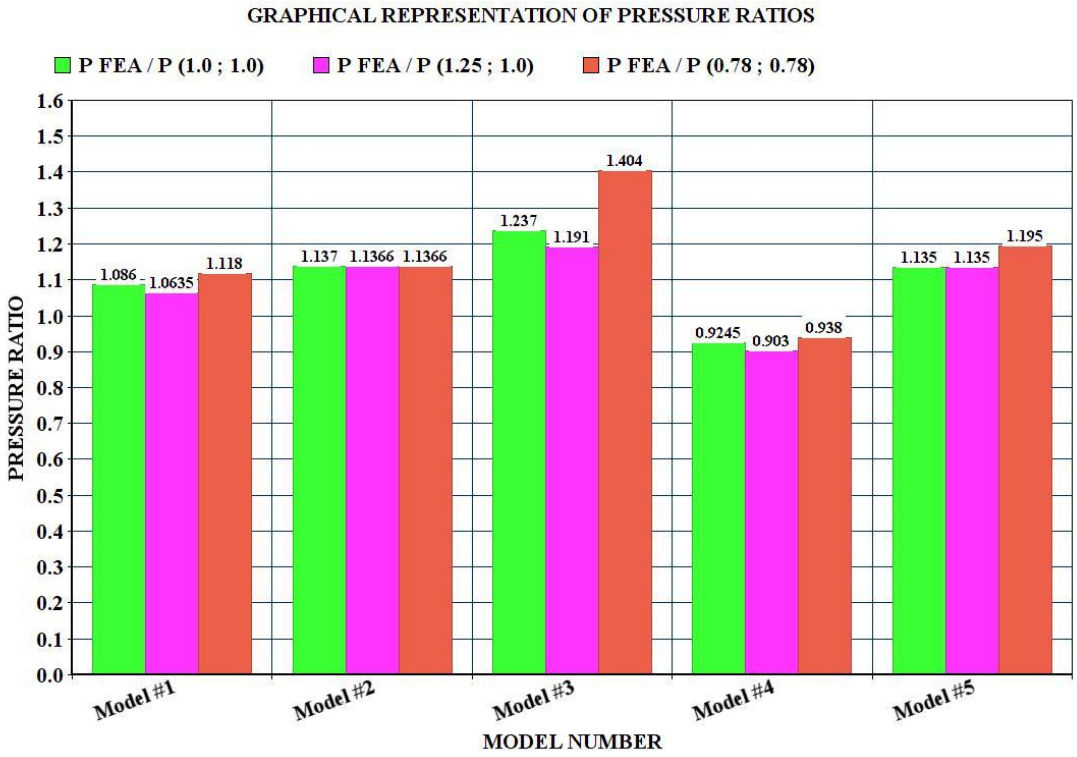
GRAPHICAL REPRESENTATION OF PRESSURE RATIOS
P FEA / P (1.0 ; 1.0)
P FEA / P (1.25 ; 1.0)
P FEA / P (0.78 ; 0.78)
PRESSURE RATIO
1.086
1.0635
1.118
1.137
1.1366
1.1366
1.237
1.191
1.404
0.9245
0.903
0.938
1.135
1.135
1.195
Model #1
Model #2
Model #3
Model #4
Model #5
MODEL NUMBER

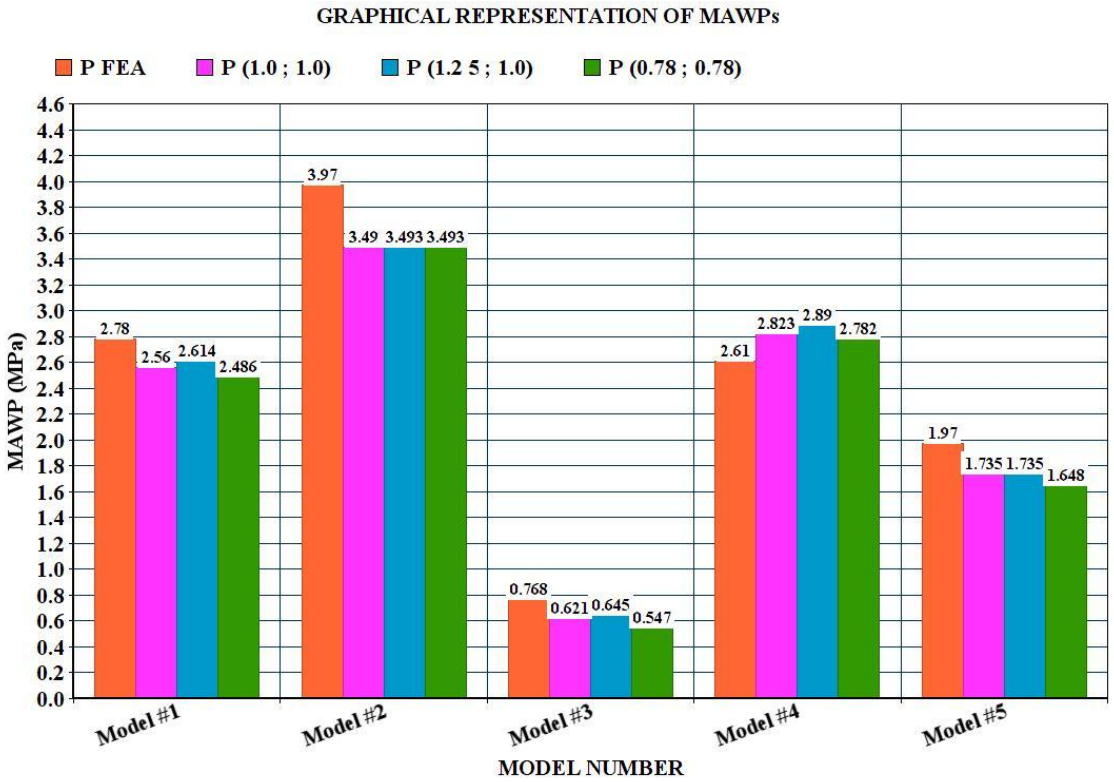
GRAPHICAL REPRESENTATION OF MAWPs
P FEA
P (1.0 ; 1.0)
P (1.2 5 ; 1.0)
P (0.78 ; 0.78)
MAWP (MPa)
2.78
2.56
2.614
2.486
3.97
3.49
3.493
3.493
0.768
0.621
0.645
0.547
2.61
2.823
2.89
2.782
1.97
1.735
1.735
1.648
Model #1
Model #2
Model #3
Model #4
Model #5
MODEL NUMBER

Observations

For the nozzles on the cylindrical shell, it appears that any randomly chosen K_N - K_S scenario yields more conservative results compared to the FEA results. The differences found lie between approximately 6% and 40%. For the nozzle on the spherical shell, the permissible internal pressure determined by FEA yields a lower value for all K_N - K_S scenarios. The differences are between approximately 7% and 11%. There is no unambiguous trend in the K_N and K_S factors that, when applying an analytical calculation, yield results that match to the FEA computations.

IV. CONCLUSIONS

Many internationally recognized codes and standards [5][6][7][8][9][10][11] etc. adopted the pressure-area method for the nozzle compensation design in pressure vessels. However, the differences between them manifest themselves to the limits of considering the pressure - loaded area and the pressure - bearing area. The K_N and K_S factors are characteristic for determining these areas. On the basis of a reasonable number of calculations performed (which by the way are not shown in this article) with varying K_N and K_S values as earlier mentioned, it can roughly be stated that the mutual differences in allowable pressure can amount to approximately 25%. The average difference between the cases examined was approximately 13%. A substantiation of the K_N and K_S factors is lacking in the cited design codes and standards. The additional FEA computations do not provide sufficient conclusive evidence for an optimal choice of the possible scenarios. Consequently, the results obtained provide ample grounds for further investigation, since it is unknown which K_N and K_S factors will lead to the most reasonable and reliable allowable internal pressures. Further research is therefore desirable to determine which K_N and K_S factors most closely approximate the FEA result and are representative of a sufficient number of nozzle-shell barrel geometries. The expectation is that as the nozzle diameter increases, the K_S factor decreases.

ACKNOWLEDGMENT

The author appreciates Keith Kachelhofer of MacAljon Fabrication / MacAljon Engineering (USA) for his cooperative attitude and efforts to prepare the manuscript.

REFERENCES

[1]. Harvey, J. F. (1985) Theory and Design of Modern Pressure Vessels, 2nd Edition, Van Nostrand - Reinhold, Princeton, N.J.
[2]. Bednar, H.H. (1981), Pressure Vessel Design Handbook, Van Nostrand - Reinhold Co., Princeton, H.J.
[3]. Pressure Vessel Design ;Spence, J. (Ed.), Tooth, A. (Ed.). (1994). Pressure Vessel Design, London: CRC Press, https://doi.org/10.1201/9781482271409
[4]. M. Hetényi, Beams on elastic foundation, Ann Arbor : The University of Michigan Press.(1976)
[5]. EN 13445-3:2014 + A8:2019 "Unfired pressure vessels" - Design
[6]. PD 5500:2018+A3:2020 "SPECIFICATION FOR UNFIRED FUSION WELDED PRESSURE VESSELS"
[7]. AD 2000 Merkblatt B9 : 2010 OPENINGS IN CYLINDRICAL, CONICAL AND SPHERICAL SHELLS
[8]. CODAP Division 2: 2015 - Revision 2018 - EN and Part C
[9]. Rules for pressure vessels, Sheet D 0501"Openings in a curved wall" Issue 03 - 2012, Sdu publishers (NL)
[10]. ASME BPVC Section VIII - Division 2, 2017 - Alternative Rules
[11]. Russian code for Pressure Vessels GOST 34233 - part 1 -12: 2017

Walther Stikvoort. "Effect of contributing shell and nozzle length on pressure capacity." *American Journal of Engineering Research (AJER)*, vol. 9(12), 2020, pp. 19-55.